1 **Middle Miocene climate of southwestern Anatolia from multiple botanical proxies**

2

3 Johannes M. Bouchal[1, 2,], Tuncay H. Güner[3,1], Thomas Denk[1]

4 [1]Department of Palaeobiology, Swedish Museum of Natural History, 10405 Stockholm,

5 Sweden

6 [2]Department of Palaeontology, University of Vienna, 1090 Vienna, Austria

7 [3]Faculty of Forestry, Department of Forest Botany, Istanbul University Cerrahpaşa, 34473

8 Bahçeköy, Istanbul, Turkey

9

10 **Correspondence to**: Johannes M. Bouchal (johannes.bouchal@nrm.se) and Thomas Denk

11 (thomas.denk@nrm.se)

12

13

14

15

Abstract

The middle Miocene climate transition (MMCT) was a phase of global cooling possibly linked to decreasing levels of atmospheric CO_2. The MMCT coincided with the European Mammal Faunal Zone MN6. From this time, important biogeographic links between Anatolia and eastern Africa include the hominid *Kenyapithecus*. Vertebrate fossils suggested mixed open and forested landscapes under (sub)tropical seasonal climates for Anatolia. Here, we infer the palaeoclimate during the MMCT and the succeeding cooling phase for a middle Miocene (14.8–13.2 Ma) intramontane basin in southwestern Anatolia using three palaeobotanical proxies: (i) Köppen signatures based on the nearest-living-relative principle. (ii) Leaf physiognomy analysed with the Climate Leaf Analysis Multivariate Program (CLAMP). (iii) Genus-level biogeographic affinities of fossil floras with modern regions. The three proxies reject tropical and hot subtropical climates for the MMCT of southwestern Anatolia and instead infer mild warm temperate *C* climates. Köppen signatures reject summer-dry *Cs* climates but cannot discriminate between fully humid *Cf* and winter-dry *Cw*; CLAMP reconstructs *Cf* climate based on the low X3.wet/X3.dry ratio. Additionally, we assess whether the palaeobotanical record does resolve transitions from the warm Miocene Climatic Optimum (MCO, 16.8–14.7 Ma) into the MMCT (14.7–13.9 Ma), and a more pronounced cooling at 13.9–13.8 Ma, as reconstructed from benthic stable isotope data. For southwestern Anatolia, we find that arboreal taxa predominate in MCO floras (MN5), whereas in MMCT floras (MN6) abundances of arboreal and non-arboreal elements strongly fluctuate indicating higher structural complexity of the vegetation. Our data show a distinct pollen zone between MN6 and MN7+8 dominated by herbaceous taxa. The boundary MN6 and MN7+8, roughly corresponding to a first abrupt cooling at 13.9–13.8 Ma, might be associated with this herb-rich pollen zone.

1 Introduction

The middle Miocene (15.97–11.63 Ma, ICS-chart 2017/02, Cohen, 2013) is characterized by a warm phase lasting until ca. 15 Ma that was followed by a gradual cooling and the restoration of a major Antarctic ice sheet and first northern hemispheric glaciations (Holbourn et al., 2014). It has been suggested that the final closure of the Mediterranean gateway connecting the Mediterranean with the Indian Ocean and the resulting changes in ocean circulation might have been one of the reasons for the final expansion of the East Antarctic ice sheet around 14.8 Ma (Flower & Kennett, 1993). During the middle Miocene climate transition (MMCT) at 14.7 to 13.8 Ma a drop of sea surface temperatures of 6–7°C occurred (Shevenell et al., 2004). At the same time, different proxies to reconstruct atmospheric CO_2 levels for the Miocene Climatic Optimum (MCO), MMCT, and the succeeding more pronounced cooling, do not concur (Beerling & Royer, 2011). Specifically, stable isotope data from phytoplankton infer stable CO_2 levels for the Neogene, with minor fluctuations (MCO, 227–327 ppm, MMCT, 265–300 ppm; see table S1 of Beerling & Royer, 2011), while stomata densities from fossil leaves suggest a pronounced drop of CO_2 after the MCO (see table S 1 of Beerling & Royer, 2011).

The European Mammal Faunal Zone MN6 (14.8–13.8 Ma; Neubauer et al., 2015) coincides with the MMCT. From this period world-famous vertebrate faunas are known from western Anatolia (e.g. Andrews & Tobien, 1977; Mayda et al., 2015) including the hominoids *Griphopithecus alpani* in Çandır and Paşalar, and *Kenyapithecus kizili* in Paşalar (Stringer & Andrews, 2011). Geraads et al. (2003) investigated the depositional environment and large mammal fauna of Çandır close to Ankara and inferred open landscapes for this locality. Bernor et al. (1979, p. 86) analysed community structure of Turkish and European middle Miocene faunas and suggested that "*faunas adapted to woodland conditions were present … at localities such as Paşalar and Yeni Eskihisar* [MN7+8]" while the "*Çandır fauna has a community structure more suggestive of closed woodland conditions*". This interpretation is

68 the exact opposite of that by Geraads et al. (2003). Recent investigations using carnivore guild

69 structure suggest a "*mixed environment between tropical forest and open savannah*

70 *landscape*s" for Çandır and Paşalar (Mayda et al., 2015). Strömberg et al. (2007) investigated

71 phytoliths (plant silica bodies) from early to late Miocene deposits of Turkey and suggested

72 that open, grass-dominated habitats had become common in Turkey and adjacent areas by the

73 early Miocene (c. 20 Ma). In contrast, Kayseri-Özer (2017) using 'integrated plant record'

74 (IPR) analysis (Kovar-Eder et al., 2008) suggested that various forest types covered most of

75 western and Central Anatolia during the middle Miocene (*broad-leaved evergreen* and *mixed*

76 *mesophytic forests* and ecotones between these forests).

77 Here we use a large data set from recently published macrofossils and pollen, spores and cysts

78 from a well-dated middle Miocene basin in western Anatolia to infer palaeoclimate and

79 palaeoenvironments using three palaeobotanical proxies: climate affinity of modern analogues

80 ('nearest living relatives'; taxon-based approach), leaf physiognomy (a-taxonomic), and

81 biogeographic affiliation of plant communities (also taxon-based). The following research

82 questions are addressed: How do the three approaches resolve local climate conditions of

83 Anatolia during a phase of global cooling, ca. 15–13 million years ago? Do different proxies

84 agree on climate inference? Where do modern climates occur that correspond to middle

85 Miocene climates of western Anatolia? Can the palaeobotanical record resolve transitions

86 between MCO, MMCT, and the succeeding more pronounced cooling during the middle

87 Miocene?

88

89 **2 Material and methods**

90 **2.1 Geological setting**

91 The Yatağan Basin is a southeast trending graben (50 km long, 15 km wide) in the province

92 of Muğla, southwestern Turkey (Fig. 1). The Neogene basin fill is up to 600 m thick and

93 divided into the Eskihisar Formation (early to middle Miocene), the Yatağan Formation (late

94   Miocene to early Pliocene), and the Milet Formation (middle to late Pliocene; Alçiçek, 2010).

95   The Eskihisar Formation comprises the Turgut Member (reddened alluvial-fan deposits

96   followed by fluviatile deposits and lignites) and the Sekköy Member (fossiliferous limnic

97   marls and limestones); all economically exploited lignite seams of the Yatağan Basin are

98   confined to the transition zone of these two members (Atalay, 1980; Becker-Platen, 1970).

99   For the present study, we investigated the palaeobotanical content (pollen and plant

100   macrofossils) of the upper Turgut and the Sekköy members exposed at the lignite mines of

101   Eskihisar, Salihpaşalar, and Tınaz (Fig. 1.2). The age of the investigated sediments is well

102   constrained by mammal fossils (Eskihisar lignite gallery locality, MN6, *Gomphotherium*

103   *angustidens* Cuvier 1817, *Percrocuta miocenica* Pavlov et Thenius 1965, Bouchal et al.,

104   2017; Yeni Eskihisar vertebrate locality, MN 7/8, The NOW Community, 2018), and by

105   radiometric dates from the upper Sekköy Member (13.2 Ma ± 0.35, Becker-Platen et al.,

106   1977). Hence, the investigated pollen zones (PZ) 1, 2, 2/3, and the Yeni Eskihisar pollen

107   assemblage represent the Neogene mammal zones MN6 and MN7+8, 14.8–13.2 Ma;

108   Neubauer et al., 2015). The layers from which most of the leaf fossils originate correspond to

109   PZ 2. A ~20 m section comprised of limestone and clayey limestone between PZ 2/3 and the

110   Yeni Eskihisar assemblage is barren of palynological content (Fig. 2).

111

112   **2.2 Plant material**

113   The investigated plant material comprises roughly 1800 macrofossils (mainly leaf fossils)

114   collected between 2010 and 2017. Macrofossils represent 77 taxa, of which five belong to

115   gymnosperms and 72 to angiosperms. Pollen, spores and cysts from five pollen zones (Fig. 2)

116   represent 182 taxa, of which one is a fungus, 9 are algae, 17 moss or fern allies spores, 15

117   gymnosperms, and 140 angiosperms (Supplementary Material S1; for taxonomic descriptions

118   of the plant taxa see Yavuz-Işık et al., 2011; Bouchal et al., 2016, 2017; Bouchal, in press;

119   Güner et al., 2017).

2.3 Köppen signatures

Fossil taxa that are resolved to genus or sectional level were represented by extant members

of the genera and sections as modern analogues. First, for accepted taxa (IPNI,

http://www.ipni.org/index.html; most recent regional floras and monographs) their

distribution ranges were determined. Then, 26 Köppen-Geiger climate types (see Table 3 for

detailed explanation of Köppen-Geiger climate types, and Kottek et al., 2006; Peel et al.,

2007; Rubel et al., 2017; Global_1986-2010_KG_5m.kmz) were mapped on modern

distribution ranges using Google Earth to establish 'Köppen signatures' (Denk et al. 2013) for

each modern analogue. Representation of different climate types was first scored for each

species within a genus as present (1)/absent (0). To summarize preferences for climate types

of all modern analogues, we used an implicit weighting scheme to discriminate between

modern analogues that are highly decisive (climatically constrained) vs. those that can be

found in many climate zones. The sum of each modern species' Köppen signature is always

one. For example, *Tilia chingiana* is present in two Köppen-Geiger climate types, *Cfa* and

Cfb, which count as 0.5 for each type , while *Tilia americana* is present in ten Köppen-Geiger

climate types (*As*, *Aw*, *Cfa*, *Cfb*, *Dfa*, *Dfb*, *Cwa*, *Cwb*, *BSk*, *BWh*), all counting as 0.1. The

Köppen signature of a genus or section, the modern analogue of a fossil taxon, is the sum of

its species' Köppen signatures for each climate type divided by the total number of scored

species for this genus. By this, the percentage representation of each Köppen-Geiger climate

type was determined for a genus/ section. In case of *Tilia*, the distribution ranges of 26 species

resulted in a genus Köppen signature as follows: *Cfa*, 22.1%, *Cfb*, 14.7%, *Cwa*, 19.9%, *Cwb*,

9.1%, *Dfb*, 5.7%, for the five most common climate types. Fig. 3.1 shows all climate types

realized in genus *Tilia*; Fig. 3.2 shows that the genus occurs predominantly in *Cf* and *Cw*

Köppen-Geiger climate types and that tropical and desert climates are nearly absent (see

145   Supplementary Material S3 for genus-level scoring of Köppen-Geiger climate types for all

146   plant taxa encountered in the Yatağan basin fossil assemblages).

147   For taxa that are resolved to family-level only, mainly pollen taxa of herbaceous and a few

148   woody angiosperm groups, the distributions of extant members of the family were combined

149   into a general family distribution range and the corresponding Köppen-Geiger climate types

150   determined.

151   Genus-level Köppen-Geiger signals were used to account for possible niche evolution within

152   lineages/ species groups of a genus. For example, modern species of *Quercus* section *Ilex* are

153   typical members of sclerophyllous, evergreen Mediterranean forest and shrubland vegetation

154   thriving under a *Cs* (summer-dry warm temperate) climate in western Eurasia and to the south

155   of the eastern Hindu Kush and Karakorum ranges, but also occur in humid, mesophytic

156   forests from Afghanistan to East Asia (*Cf* and *Cw* climates). To account for this climate niche

157   variability, all species of sect. *Ilex* were scored for the general Köppen signature of sect. *Ilex*.

158   Hence, the entire section was used as modern analogue, the nearest living relative (NLR), for

159   several fossil species of *Quercus* sect. *Ilex*.

160

161   **2.4 CLAMP**

162   We inferred quantitative palaeoclimate parameters for the three Yatağan Basin floras using

163   the Climate Leaf Analysis Multivariate Program (CLAMP) (Yang et al., 2011). CLAMP

164   makes use of the relationship between leaf physiognomy of dicotyledonous flowering plants

165   and climate and, hence, is a non-taxonomic approach to palaeoclimate inference (Spicer,

166   2008). CLAMP calibrates the numerical relations between leaf physiognomy of woody

167   dicots and meteorological parameters in modern terrestrial environments. With this

168   calibration, past climatic data can be determined from leaf fossil assemblages if the

169   sampling of the fossil assemblage represents well the characteristics of the living source

170   vegetation (http://clamp.ibcas.ac.cn). Modern and fossil leaf physiognomic data are

171 positioned in multidimensional physiognomic space using canonical correspondance analysis

172 (CANOCO; Ter Braak, 1986). CANOCO orders vegetation sites based on a set of attributes

173 (leaf physiognomic characters).

174 For modern sites, climate variables are known from long-term observations of climate stations

175 or from high-resolution gridded climate data (New et al., 1999, 2002; Spicer et al., 2009).

176 Vectors for each of the measured climate variables can be positioned in physiognomic space

177 and calibrated. Palaeoclimate variables can then be quantified by scoring a fossil assemblage

178 in the same manner as for the modern vegetation and positioning the fossil site in

179 physiognomic space (http://clamp.ibcas.ac.cn).

180 For the present study, 36 different leaf characters (including leaf shape and size, apex shape,

181 base shape, and leaf margin characteristics) were scored for 61, 63, and 14 dicotyledonous

182 leaf morphotypes from three localities, Tınaz, Eskihisar, and Salihpaşalar (see Supplementary

183 Material S3 for scoring of morphotypes), following the CLAMP protocols

184 (http://clamp.ibcas.ac.cn). At genus level, the floras of the Yatağan Basin show highest

185 similarity with Eurasian extant woody angiosperms (Table 1), thus the PhysgAsia1

186 Calibration files dataset of CLAMP was used to position the fossil data.

187

188 *2.5 Genus level biogeographic affinities*

189 For all fossil taxa determined to genus level, the present distribution was tabulated indicating

190 presence/absence of a genus in western Eurasia, East Asia, eastern North America, western

191 North America, and Africa (Table 1).

192

193 **3 Results**

194 **3.1 Climate inference from Köppen signatures** (Fig. 5, Supplementary Materials S4, S5)

195 For the fossil plant assemblages warm temperate to temperate *C* and *D* climates accounted for

196 almost 80% of the realized Köppen-Geiger climate types of all taxa in a fossil plant

197 assemblage (using genus-level NLR). The sum of *Cf*, *Df*, *Cw* and *Dw* climates amounted to

198 60–70% in all assemblages (highest scores in macrofossil assemblages).

199 Overall, the best represented Köppen-Geiger climate types when using genus-level NLR were

200 *Cfa* (warm temperate, fully humid, hot summer), followed by *Cfb* (warm temperate, fully

201 humid, warm summer), *Cwa* (warm temperate, winter-dry, hot summer), and *Cwb* (warm

202 temperate, winter-dry, warm summer). Summer-dry *Cs* climates were represented by 9–13%

203 and arid (generally dry) *B* climates by 6–11% (Table 3, Supplementary Materials S4).

204 Tropical (equatorial) climates (*A*) are represented by 9–11% in older assemblages, and 7–8%

205 in the two youngest assemblages (PZ 2/3 and Yeni Eskihisar). Of 1555 modern species used

206 to inform the Köppen signatures of the NLRs for the fossil taxa, 119 show marginal range

207 extensions into *Af* climate, 168 into *Am* (heavy monsoon), 85 into *As*, and 295 into *Aw*

208 (Supplementary Material S2). Taxa extending in tropical climates are mainly species of *Pinus*,

209 *Celtis*, *Smilax*, and *Viburnum*, *Quercus* sections *Quercus* and *Lobatae*, Juglandaceae

210 subfamily Engelhardioideae, Oleaceae, and Sapotaceae. Exclusion of Köppen-Geiger climate

211 signals extracted from cosmopolitan and/or gymnospermous taxa did not change the general

212 trends (Supplementary Material S5).

213

214 **3.2 CLAMP**

215 Sixty-three morphotypes were scored for Eskihisar (Fig. 6; see Supplementary Material S3 for

216 score sheets and other reconstructed climate parameters). Inferred values for mean annual

217 temperature (MAT) were (11.2–) 12.6 (–14) °C, for coldest month mean temperature

218 (CMMT) (0.3–) 2.3 (–4.4) °C, and for the three wettest months (X3.wet) (410–) 666 (–936)

219 mm and for the three driest months (X3.dry) (148–) 204 (–262) mm. The ratio X3.wet/X3.dry

220 was between 2.9 and 3.6. For Tınaz, the reconstructed MAT was (12.3–) 13.8 (–15.2) °C,

221 CMMT (1.5–) 3.6 (–5.6) °C, X3.wet (420–) 700 (–980) mm, and X3.dry (146–) 205 (–260)

222 mm. The ratio X3.wet/X3.dry was between 2.9 and 3.8. Values for Salihpaşalar are not

223 considered here as they are based on a too small set of morphotypes (see Supplementary

224 Material S3).

225

226 **3.3 Genus level biogeography**

227 The genus-level biogeographic analysis of the four Yatağan Basin floras ranging in age from

228 14.8 to 13.2 Ma (MN6 into MN7+8; Table 1) shows that closest biogeographic relationships

229 are with the modern East Asian flora (54 of 59 taxa shared with East Asia), 48 and 44 genera

230 are shared with the modern western Eurasian and eastern North American floras, respectively.

231 Among modern tropical floras, closest relationships are with South America (21), followed by

232 Africa (16) and northern/ north-eastern Australia (13). Most taxa extending to tropical regions

233 are cosmopolitan (e.g. *Euphorbia*, *Drosera*, *Phragmites*), hence, of little discriminative

234 power. This is also true for higher taxa such as Polygalaceae and Valerianoideae. The fossil

235 species *Smilax miohavanensis* belongs to a subtropical-tropical clade of extant species (Denk

236 et al., 2015) and is the only member of this group in Eurasia; it has its last occurrence in the

237 middle Miocene floras of the Yatağan Basin. Overall, the dominating biogeographic signal is

238 a northern hemispheric one.

239

240 **3.4 Changes in ratios arboreal to non-arboreal pollen**

241 Ratios of arboreal pollen (AP) to non-arboreal pollen (NAP) change considerably among and

242 within pollen zones of the Yatağan Basin assemblages (Table 2, Supplementary Material S6).

243 Pollen zone 1 (main lignite seam) consistently has high percentages of AP (94–70%). In

244 contrast, AP percentage values fluctuate throughout pollen zone 2, with values from 89 to 29.

245 Pollen zone 2-3, only covered in the Tınaz section, records AP percentages of 50 to 19.

246 Above, the MN7+8 assemblage of Yeni Eskihisar shows again a higher proportion of arboreal

247 taxa (67%). Similarly, from the vertebrate locality Çatakbağyaka (revised age MN7+8, 12 km

248 south of the Yatağan Basin) AP percentages range from c. 50% to c. 80% (Jiménez-Moreno,

249 2005; Mayda et al., 2016; Bouchal et al. 2017; Aiglstorfer et al. 2018).

250 We used the threshold (AP/NAP = 3.85) proposed by Favre et al. (2008) to separate between

251 tree- and herb-prevalent environments. This ratio translates into AP percentages of close to

252 80% to predict reliably tree-prevalent landscapes. As can be seen in Supplementary Material

253 S6, pollen zones 1 and 2 are largely dominated by forested environments. In the upper part of

254 PZ2 (Tınaz, Eskihisar), PZ2/3 and PZ3 (Tınaz) herb-prevalent landscapes are inferred.

255 However, it is noteworthy, that although NAP taxa are more abundant in these pollen zones,

256 AP taxa remain to have fairly high percentages as well (Bouchal et al., 2016, 2017). For

257 example, *Fagus*, *Quercus* deciduous and evergreen type, still are above the threshold values

258 indicative of local tree presence (Lisitsyna et al., 2011). Hence, the opening of the vegetation

259 in the upper parts of PZ2, and in PZ2/3, PZ3 may actually represent a coexistence of forest

260 and open vegetation.

261

262 **4 Discussion**

263 **4.1 Climate inference using Köppen signatures and CLAMP**

264 Using Köppen signatures, we made a semi-quantitative reconstruction of the palaeoclimate of

265 the Yatağan Basin during the middle Miocene. All Köppen signatures used here rely on the

266 nearest-living-relative principle (Denk et al., 2013). Such approaches are prone to error

267 because niche evolution may have occurred in lineages, the morphologically nearest living

268 relatives (NLRs), a species or group of morphologically similar species, of fossil taxa may

269 have different niches, and the shift is difficult to quantify (Ackerly, 2004; Grimm & Potts,

270 2016; Denk et al., 2017). Hence, we opted against applying quantitative NLR methods and

271 determined Köppen signatures for fossil taxa using information from all extant species of a

272 genus used as NLR to avoid bias from undetected niche shifts.

273 It is important to keep climatic niche shift in mind when using NLR based approaches to

274 palaeoclimate inference and interpreting their results (cf. Grimm & Potts, 2016; Denk et al.,

275 2017). In our dataset of 1555 modern species, 295 also occur in tropical *Aw* climates. Most of

276 them belong to clades (monophyletic sections, genera, families) that occur in a wide range of

277 climate types (e.g. Amaranthaceae, *Celtis*, white and red oaks). Others, such as *Engelhardia*

278 are usually interpreted as tropical-subtropical evergreen element (Kvaček, 2007) based on the

279 distribution range of the extant genera of the comprising subfamily, the Engelhardoideae.

280 However, '*Engelhardia*' of the western Eurasian Cenozoic belongs to its own (extinct)

281 section or genus *Palaeocarya* (Kvaček, 2007) with a stratigraphic range from Eocene to

282 Pliocene. Pollen, foliage, and reproductive structures of fossil material clearly belong to

283 subfamily Engelhardioideae but cannot be assigned to just a single modern genus *Engelhardia*

284 (tropical Southeast Asia). Instead the fossil-taxon is a mosaic taxon having characteristics of

285 both American and Asian members of the subfamily. Kvaček (2007) noted that the fossil

286 genus/subgenus flourished in subtropical climates during the Eocene but in distinctly

287 temperate climates with coldest month mean temperatures close to the freezing point in the

288 Neogene, in stark contrast to the surviving four, likely relict genera of the Engelhardioideae.

289 Hence, this extinct lineage of Engelhardioideae is not well represented by a single or the

290 combination of all extant genera and their constituent species. Similarly, representatives of

291 *Smilax havanensis* and allied species are part of a New World clade with most species

292 occurring in tropical climates. However, the single Old World member of the clade, the fossil

293 species *S. miohavanensis*, is known from early to middle Miocene strata of Anatolia and

294 Central Europe (Denk et al., 2015). This fossil species formed part of plant assemblages that

295 rule out tropical climates. In this case, inferring palaeoclimate from extant distribution data

296 only inevitably will produce noise to the climatic signal.

297 Overall, the most common Köppen-Geiger climate types of NLR taxa of the Yatağan floras

298 were warm temperate *C* types, and among *C* types fully humid *Cf* climates were better

299　represented than more seasonal *Cw* and *Cs* types (Fig. 5; Supplementary Material S4). *Cs*

300　types played only a minor role; however, there was no clear preference of *Cf* over *Cw*

301　climates in the representation of Köppen-Geiger climate types. Removing azonal taxa, or taxa

302　commonly associated with higher elevations (conifers) did not affect the general signal.

303　In contrast, CLAMP is not based on NLR and hence not potentially biased by taxonomic

304　error. Its combination with the Köppen signature analysis provides a powerful tool for climate

305　inference and to discern between seasonal *Cw* (winter dry) and *Cs* (summer dry) and fully

306　humid *Cf* climates can be made. Specifically, the ratio of the wettest and the driest month

307　clearly distinguishes strongly seasonal summer rain (monsoon) climates (*Cw*; precipitation

308　wettest month > 10x precipitation driest month, $[P_{wdry/sdry} < P_{wet/wwet}/10]$; Peel et al., 2007)

309　from weakly seasonal, fully humid climates (*Cf*; precipitation wettest month << 10x

310　precipitation driest month). Precipitation values for X3.wet and X3.dry inferred by CLAMP,

311　and the ratio between these ranges being between 2.9 and 3.8 thus largely rules out a *Cw*

312　climate (X3.wet and X3.dry are closely correlated to $P_{dry/wet}$). In conjunction with the Köppen

313　signature results ruling out summer-dry conditions, the CLAMP precipitation and temperature

314　estimates point towards cold subtropical to mild temperate *Cfa* climates at the margin to fully

315　temperate *Cfb* climates.

316

317　**4.2 Comparison to palaeoclimate and palaeoenvironment inferences from other proxies**

318　A further refinement of previous climate and vegetation inferences can be made regarding the

319　distinction between tropical ($T_{min} \equiv CMMT \geq 18 °C$), subtropical (8–12 months with $T \geq 10°$

320　C; ~ MAT 12–18 °C, and CMMT <18 °C) and temperate climates. CLAMP consistently

321　resolves MAT < 18 ºC and CMMT < 6 °C for the localities Eskihisar and Tınaz, and this

322　agrees with the results from Köppen signatures and a previous qualitative assessment of

323　palaeoenvironments in the Yatağan Basin (Güner et al., 2017). Both these results, rejecting

324　strongly seasonal *Cw* climates, summer dry *Cs,* and tropical *A* climates (at least for non-

13

coastal areas) for the middle Miocene of western Anatolia, have implications for the

reconstruction of palaeoenvironments of famous vertebrate localities in Anatolia that are

assigned to MN6. The $\delta^{13}C$ composition from fossil tooth enamel at Paşalar, western

Anatolia, MN6, indicates that animals were feeding on C_3 vegetation (Quade et al., 1995).

The palaeoenvironment for this locality was determined as closer to Indian subtropical

forests, with seasonal summer rainfalls (i.e. warm *Cwa* climates), semi-deciduous forest and

dense ground vegetation (Stringer & Andrews, 2011; Mayda et al., 2015). Using carnivore

guild structures Morlo et al. (2010) inferred open (Serengeti type, *Aw* climate) landscapes for

the Central Anatolian MN6 vertebrate locality Çandır. Also, the NOW database

(http://www.helsinki.fi/science/now/; The NOW Community, 2018) refers to Çandır as more

open ("woodland biome", "open vegetation structure", "grassland with mosaic of forests")

and to Paşalar as more forested landscapes ("subtropical", "closed vegetation structure",

"semi-deciduous forests"). Bernor et al. (1979) using community structure of vertebrate

faunas inferred densely wooded environments for Çandır. In a later study based on a

taxonomic revision of carnivores, Mayda et al. (2015) proposed a mixed environment

between tropical forests and open savannah landscapes for Çandır. It is important to note that

these carnivore guild structure studies used only two modern calibration faunas to estimate

palaeoenvironments, one tropical rainforest fauna in Guyana, and one savannah (tropical)

fauna in the Serengeti (Morlo et al., 2010). Thus, using this proxy, only two environments can

be reconstructed, tropical savannah or rainforest.

Our plant-proxy based climate reconstruction unambiguously rejects a tropical climate for the

middle Miocene Yatağan Basin and major biogeographic patterns strongly suggest northern

hemispheric affinities. Similar environmental conditions as reconstructed in our study have

been inferred for most of western Anatolia during the late early and middle Miocene

(Kayseri-Özer, 2017). Most proxies currently used to infer climate and vegetation in western

Anatolia during the middle Miocene (carnivore guild structures, vertebrate community

351 structure, plant functional types, plant macrofossils, pollen and spores; Mayda et al., 2015,

352 2016; Kayseri-Özer, 2017; Güner et al., 2017; Bouchal et al. 2016, 2017; Bouchal, 2018)

353 clearly infer forested vegetation with varying contributions of open vegetation. In contrast,

354 Strömberg et al. (2007) found that "*all Miocene phytolith assemblages point to relatively open*

355 *vegetation, such as savanna or open woodland dominated by open-habitat grasses, or a*

356 *mixture of grassland and wooded areas*". This result may be biased (see Jokela, 2015, p. 44)

357 and increased diversity of grass types in the phytolith record may not necessarily indicate the

358 presence of widespread open, grass-dominated landscapes.

359

360 **4.3 Modern climate analogues**

361 The inferred climate for the middle Miocene Yatağan Basin plant assemblages is

362 characterized by MAT 11–15 °C, coldest month mean temperature (CMMT) 0–6 °C, MAP

363 ca. 1000–2000 mm, and ratios of X3.wet/X3.dry 2.9–3.8. A non-exhaustive search for climate

364 stations with this combination of climate parameters (Supplementary Material S7) identified a

365 single closest match, Pacific central Honshu of Japan. X3.wet/X3.dry ratios and MAT are

366 similar to the upper limits of the ranges reconstructed for the middle Miocene Yatağan Basin.

367 East Asian *Cf* climates are generally characterized by distinct summer rain maxima. The

368 modern vegetation of Japan is home to many plant taxa that are currently absent from western

369 Eurasia but were abundant in Neogene plant assemblages of western Eurasia (e.g.

370 *Cephalotaxus, Cryptomeria, Torreya, Alangium, Camellia, Castanopsis, Cercidiphyllum,*

371 *Daphniphyllum, Eurya, Fatsia*; Mai, 1995; Miyawaki, 1984; see also Milne, 2004). These

372 taxa require warm and humid equable climates.

373 A further close match is the area from northern Turkey via Georgia to northern Iran, the

374 Euxinian-Hyrcanian region (Supplementary Material S7). Climates at the transition between

375 *Csa* and *Cfa/b* of the region north of Istanbul have up to 1166 mm MAP (Ustaoğlu, 2012) and

376 other climate parameters in this area match the Miocene climate of southwestern Turkey

inferred by CLAMP. Towards the humid north-eastern part of Turkey, X3.wet/X3.dry ratios

are lower (2.4 for Rize, Hopa and Poti and Kobuleti in adjacent western Georgia). Further to

the east, south of the Caspian Sea, Rasht and Kiashahr have *Cfa* and borderline *Csa* to *Cfa*

climates with slightly more pronounced seasonality than the reconstructed climate for the

Miocene of southwestern Turkey (X3.wet/X3.dry ratios 4.4 and 4.2). In contrast,

X3.wet/X3.dry ratios in modern Mediterranean western and southwestern Turkey amount to

25 (Izmir) and 21.8 (Muğla, Yatağan Basin). It is noteworthy that modern *Cf* climates of the

Euxinian-Hyrcanian region differ markedly from those of the Pacific part of Honshu by their

summer minima in rainfall (Supplementary Material S7). This feature indicates a (weak)

Mediterranean influence in this region. According to Biltekin et al. (2015) the Anatolian

refugium emerged after the retreat of the Paratethys Sea in the Pliocene and increasing

monsoon influence (increased summer rainfall) over the north-eastern Mediterranean region

(the latter accounting for the much higher summer precipitation in the Euxinian-Hyrcanian

than in the Mediterranean region). The Mediterranean climate type in Europe appeared first

during the late Pliocene and early Pleistocene (ca. 3.2–2.3 Ma; Suc, 1984) coinciding with

first large-scale north hemispheric glaciation in the North Atlantic (Denk et al., 2011).

4.4 Detection of Miocene global climatic changes in the terrestrial fossil record

High-resolution benthic stable isotopic data provide a detailed chronology of (global) climatic

changes across the Miocene Climatic Optimum (MCO), the middle Miocene Climatic

transition (MMCT), and the subsequent more pronounced cooling (Holbourn et al., 2014).

The terrestrial record usually does not provide the same temporal resolution but allows

focussing on regional patterns. The transition from MCO to MMCT has previously been

documented in high-resolution palynological analyses. For example, Jiménez-Moreno et al.

(2005) investigated a core from the Pannonian Basin and observed a decline of megathermic

taxa at the transition MCO to MMCT. Also Ivanov & Worobiec (2017) reported a decrease of

403 thermophile taxa for the transition for Bulgaria and Poland. In southwestern Anatolia, Kayseri

404 et al. (2014) investigated three localities in the Muğla-Ören area south of the Yatağan Basin,

405 which are dated by vertebrate fossils as early and late MN5 and thus correspond to the MCO.

406 These authors report a few warmth-loving elements (palms, *Avicennia*) that are missing in the

407 younger strata of the Yatağan Basin. This could be due to the deltaic setting of these floras as

408 opposed to the intramontane setting of the Yatağan Basin floras. In general, the floras of the

409 Muğla-Ören area are very similar to the floras of the Yatağan Basin (Bouchal. et al., 2017).

410 However, a striking difference with the MN6 and MN7+8 assemblages of the Yatağan Basin

411 is the almost entire absence of herbaceous taxa (non-arboreal pollen) in the MN5 assemblages

412 of Ören (see figs 7–9 in Kayseri et al. 2014). This may indicate the presence of more closed

413 forest vegetation of the laurisilva type. The extant laurisilva or laurel forest is a type of

414 subtropical forest found in areas with high humidity and relatively stable, mild temperatures.

415 The assemblages of the Yatağan Basin, show fluctuating arboreal to non-arboreal pollen

416 (AP:NAP) ratios with a peak of NAP in the transition zone MN6 to MN7+8 (pollen zone PZ

417 2–3). This peak could possibly correspond to a sharp cooling detected in the benthic stable

418 isotopic data at 13.9–13.8 Ma (Holbourn et al., 2014). In the European mammal stratigraphy

419 (Neubauer et al., 2015) the boundary MN6 to MN7+8 is at 13.9 Ma. Above PZ 2–3, the

420 radiometrically dated Yeni Eskihisar pollen assemblage clearly belongs to MN7+8. Here, and

421 in the nearby locality Çatakbağyaka woody taxa (including some warmth-loving taxa) are

422 again more prominent. Thus, although the correlation of pollen zone 2–3 with the cooling

423 event at 13.9–13.8 Ma is highly speculative, it is clear that the MCO in southwestern Anatolia

424 was characterized by laurisilva vegetation with little contribution of herbaceous taxa. During

425 the MMCT the main woody taxa did not change much, but herbaceous taxa played a much

426 greater role. This indicates higher structural complexity of the vegetation. The presence of

427 early hominids in western Anatolia during this time might be connected to this more complex

428 vegetation. It is unclear at present, whether these changes were accompanied by changes in

429 concentrations of atmospheric CO_2. The compilation of reconstructed CO_2 values across the

430 Cenozoic from hundreds of proxy data (Beerling & Royer, 2011) shows that there is no

431 agreement between different proxies for the MCO and the subsequent middle Miocene

432 climate cooling. Phytoplankton stable isotopic data suggest nearly stable CO_2 concentrations

433 (MCO, 227–327 ppm, MMCT, 265–300 ppm; see table S 1 of Beerling & Royer, 2011). In

434 contrast, stomata densities from fossil leaves suggest a pronounced decline of CO_2 across this

435 interval.

436

437 **5. Conclusion**

438 Here we used three proxies to infer climate, palaeoenvironments and biogeographic affinities

439 of three middle Miocene floras of southwestern Anatolia. We showed that the palaeobotanical

440 record resolves transitions from the warm MCO (16.8–14.7 Ma) into the MMCT (14.7–13.9

441 Ma), and a more pronounced cooling at 13.9–13.8 Ma, mainly expressed in the changing and

442 fluctuating ratios between AP and NAP taxa. Using threshold percentages for main tree taxa,

443 we further show that although NAP values significantly increased during the MMCT, AP taxa

444 remained relatively abundant, signifying the coexistence of forested and open landscapes

445 during this transition. In addition, the biogeographic analysis indicates mainly northern

446 hemispheric biogeographic affinities of the middle Miocene flora of southwestern Anatolia

447 and thus invalidates previous comparisons with tropical environments. Tropical climate

448 conditions are also rejected by the Köppen signatures of the investigated floras and by the

449 CLAMP analysis. Finally, the CLAMP data readily distinguish between strongly seasonal Cs

450 and Cw and fully humid Cf climate types. More combined macrofossil and microfossil studies

451 are needed for the Neogene of Turkey in order to establish a robust framework of terrestrial

452 climate evolution in this important region.

453

454

465 **References**

466 Ackerly, D. D.: Adaptation, niche conservatism, and convergence: comparative studies of leaf
467   evolution in the California chaparral, Am. Nat., 163, 654–671, 2004.
468 Aiglstorfer, M., Mayda, S., and Heizmann, E. P. J.: First record of if late Miocene Moschidae
469   from Turkey: *Micromeryx* and *Hispanomeryx* from Catakağyaka (Muğla, SW Turkey),
470   Comptes Rendus Palevol., 17, 178–188, 2018.
471 Alçiçek, H.: Stratigraphic correlation of the Neogene basins in southwestern Anatolia:
472   Regional palaeogeographical, palaeoclimatic and tectonic implications, Palaeogeogr.
473   Palaeoclimatol. Palaeoecol. 291, 297–318, 2010.
474 Andrews, P. and Tobien, H.: New Miocene locality in Turkey with evidence on the origin of
475   *Ramapithecus* and *Sivapithecus*, Nature, 268, 699–701, 1977.
476 Atalay, Z.: Muğla-Yatağan ve yakın dolayı karasal Neojen'inin stratigrafi araştırması, Bull.
477   Geol. Soc. Turkey, C23, 93–99, 1980.
478 Becker-Platen, J. D.: Lithostratigraphische Untersuchungen im Känozoikum Südwest-
479   Anatoliens (Türkei) (Känozoikum und Braunkohlender der Türkei, 2), Beih. Geol. Jb.,
480   97, 1–244, 1970.
481 Becker-Platen, J. D., Benda, L., and Steffens, F.: Litho- und biostratigraphische Deutung
482   radiometrischer Altersbestimmungen aus dem Jungtertiär der Türkei, Geol. Jb., B25,
483   139–167, 1977.
484 Beerling, D.J., and Royer, D.L.: Convergent Cenozoic CO_2 history. Nature Geoscience, 4,
485   418–420, 2011.
486 Bell, B.A., and Fletcher, W.J.: Modern surface pollen assemblages from the Middle and High
487   Atlas, Morocco: insights into pollen representation and transport. Grana, 55, 286–301,
488   2016. http://dx.doi.org/10.1080/00173134.00172015.01108996.
489 Bernor, R.L., Andrews, P.J., Solounias, N., and Van Couvering, J.A.H.: The evolution of
490   "Pontian" mammal faunas: some zoogeographic, palaeoecologic and
491   chronostratigraphic considerations. Annales Géologiques des Pays Helléniques. Tome
492   hors série [special issue] 1979, 1, 81–89, 1979.

Biltekin, D., Popescu, S.-M., Suc, J.-P., Quézel, P., Jiménez-Moreno, G., Yavuz-Işık, N., and Çağatay, M. N.: Anatolia: A long-time plant refuge area documented by pollen records over the last 23 million years, Rev. Palaeobot. Palynol., 215, 1–22, 2015.

Bouchal, J. M.: The middle Miocene palynofloras of the Salihpaşalar lignite mine (Yatağan Basin, southwest Anatolia): environmental characterisation and comparison with coeval palynofloras from adjacent subbasins, Palaeobio. Palaeoen., in Press, 1–46, 2018. https://doi.org/10.1007/s12549-018-0345-0.

Bouchal, J. M., Mayda, S., Grímsson, F., Akgün, F., Zetter, R., and Denk, T.: Miocene palynofloras of the Tınaz lignite mine, Muğla, southwest Anatolia: taxonomy, palaeoecology and local vegetation change, Rev. Palaeobot. Palynol., 243, 1–36, 2017.

Bouchal, J. M., Zetter, R., Grímsson, F., and Denk, T.: The middle Miocene palynoflora and palaeoenvironments of Eskihisar (Yatağan Basin, southwestern Anatolia): a combined LM and SEM investigation, Bot. J. Linn. Soc., 182, 14–79, 2016.

Cohen, K.M., Finney, S.C., Gibbard, P.L., and Fan, J.-X. The ICS International Chronostratigraphic Chart, *Episodes* 36:199–204, 2013 (updated 2017). http://www.stratigraphy.org/index.php/ics-chart-timescale

Corbett, S. L. and Manchester, S. R.: Phytogeography and fossil history of *Ailanthus* (Simaroubaceae), International Journal of Plant Sciences, 165, 671–690, 2004.

Denk, T., Grimm, G. W., Grímsson, F., and Zetter, R.: Evidence from "Köppen signatures" of fossil plant assemblages for effective heat transport of Gulf Stream to subarctic North Atlantic during Miocene cooling, Biogeosciences, 10, 7927–7942, 2013.

Denk, T., Grímsson, F., Zetter, R., and Símonarson, L. A.: Late Cainozoic Floras of Iceland: 15 Million Years of Vegetation and Climate History in the Northern North Atlantic, Springer, Heidelberg, New York, 2011.

Denk, T., Velitzelos, D., Güner, H. T., Bouchal, J. M., Grímsson, F., and Grimm, G. W.: Taxonomy and palaeoecology of two widespread western Eurasian Neogene sclerophyllous oak species: *Quercus drymeja* Unger and *Q. mediterranea* Unger, Rev. Palaeobot. Palynol., 241, 98–128, 2017b.

Denk, T., Velitzelos, D., Güner, H. T., and Ferrufino-Acosta, L.: *Smilax* (Smilacaceae) from the Miocene of western Eurasia with Caribbean biogeographic affinities, Am. J. Bot., 102, 423–438, 2015.

Favre, E., Escarguel. G., Suc, J.-P., Vidal. G., and Thévenod, L.: A contribution to deciphering the meaning of AP/NAP with respect to vegetation cover, Rev. Palaeobot. Palynol., 148, 13–35, 2008.

Flower, B. P. and Kennett, J. P.: Middle Miocene deepwater paleoceanography in the southwest Pacific: relations with East Antarctic Ice Sheet development, Paleoceanography, 10, 1095–1112, 1995.

Geraads, D., Begun, D., and Güleç, E.: The middle Miocene hominoid site of Çandir, Turkey: general palaeoecological conclusions from the mammalian fauna, Courier Forschungs-Institut Senckenberg, 240, 241–250, 2003.

Grimm, G. W. and Potts, A. J.: Fallacies and fantasies: the theoretical underpinnings of the Coexistence Approach for palaeoclimate reconstruction, Clim. Past, 12, 611–622, 2016.

Güner, H. T., Bouchal, J. M., Köse, N., Göktaş, F., Mayda, S., and Denk, T.: Landscape heterogeneity in the Yatağan Basin (southwestern Turkey) during the middle Miocene inferred from plant macrofossils, Palaeontogr. B, 296, 113–171, 2017.

Holbourn, A., Kuhnt, W., Lyle, M., Schneider, L., Romero, and O., Andersen, N.: Middle Miocene climate cooling linked to intensification of eastern equatorial Pacific upwelling. Geology, 42, 19–22, 2014.

Inaner, H., Nakoman, E., and Karayigit, A. I.: Coal resource estimation in the Bayir field, Yatağan-Muğla, SW Turkey, Energy Sources A, 30, 1005–1015, 2008.

Ivanov, D. and Worobiec E.: Middle Miocene (Badenian) vegetation and climate dynamics in Bulgaria and Poland based on pollen data, Palaeogeogr. Palaeoclimatol. Palaeoecol., 467, 83–94, 2017.

Jia, L.-B., Manchester, S. R., Su, T., Xing, Y.-W., Chen, W.-Y., Huang, Y.-J., and Zhou, Z.-K.: First occurrence of *Cedrelospermum* (Ulmaceae) in Asia and its biogeographic implications, J. Plant Res., 128, 747–761, 2015.

Jiménez-Moreno, G. (2005). Utilización del análisis polínico para la reconstrucción de la vegetación, clima y estimación de paleoaltitudes a lo largo de arco alpino europeo durante el Mioceno (21–8 Ma), PhD Thesis University Granada, Granada, 313 pages.

Jiménez-Moreno, G., Rodríguez-Tovar, F.-J., Pardo-Igúzquiza, E., Fauquette, S., Suc, J.-P., Müller, P.: High-resolution palynological analysis in late early-middle Miocene core from the Pannonian Basin, Hungary: climatic changes, astronomical forcing and eustatic fluctuations in the Central Paratethys, Palaeogeogr. Palaeoclimatol. Palaeoecol., 216, 73–97, 2005.

Jokela, T.: The high, the sharp and the rounded: paleodiet and paleoecology of Late Miocene herbivorous mammals from Greece and Iran. PhD thesis, University of Helsinki, 2015. http://urn.fi/URN:NBN:fi-fe2017112252491.

Kayseri-Özer, M. S.: Cenozoic vegetation and climate change in Anatolia — A study based on the IPR-vegetation analysis, Palaeogeogr. Palaeoclimatol. Palaeoecol., 467, 37–68, 2017.

Kayseri-Özer, M.S., Akgün, F., Mayda, S., Kaya, T.: Palynofloras and vertebrates from Muğla-Ören region (SW Turkey) and palaeoclimate of the Middle Burdigalian–Langhian period in Turkey. Bull. Geosci. 89, 137–162, 2014.

Kottek, M., Grieser, J., Beck, C., Rudolf, B., and Rubel, F.: World map of the Köppen-Geiger climate classification updated., Meteorol. Z., 15, 259–263, 2006.

Kovar-Eder, J., Jechorek, H., Kvaček, Z., and Parashiv, V.: The Integrated Plant Record: An essential tool for reconstructing Neogene zonal vegetation in Europe, Palaios, 23, 97–111, 2008.

Kvaček, Z.: Do extant nearest relatives of thermophile European Cenozoic plant elements reliably reflect climatic signal?, Palaeogeogr. Palaeoclimatol. Palaeoecol., 253, 32–40, 2007.

Kvaček, Z., Velitzelos, D., and Velitzelos, E.: Late Miocene Flora of Vegora, Macedonia, N. Greece, Korali Publications, Athens, 2002.

Lisitsyna, O.V., Giesecke, T., and Hicks, S.: Exploring pollen percentage threshold values as an indication for the regional presence of major European trees, Rev. Palaeobot. Palynol., 166, 311–324, 2011.

Magri, D., Di Rita, F., Aranbarri, J., Fletcher, W., González-Sampériz, P.: Quaternary disappearance of tree taxa from Southern Europe: Timing and trends, Quat. Sci. Rev. 163,23–55, 2017.

Mai, D.H. Tertiäre Vegetationsgeschichte Europas. Jena: Gustav Fischer Verlag, 1995.

Martinetto, E.: The role of central Italy as a centre of refuge for thermophilous plants in the late Cenozoic, Acta Palaeobot., 41, 299–319, 2001.

Mayda, S., Kaya, T., and Aiglstorfer, T. M.: Revisiting the middle Miocene (MN7/8) fauna of Catakağyaka (Mugla, SW Turkey), in: Taking the orient express: RCMNS Workshop on the role of Anatolia in Mediterranean Neogene Palaeobiogeography, Izmir 16–18 Sept., 2016.

Mayda, S., Koufos, G. D., Kaya, T., and Gul, A.: New carnivore material from the Middle Miocene of Turkey. Implications on biochronology and palaeoecology, Geobios, 48, 9–23, 2015.

Milne, R. I.: Phylogeny and biogeography of *Rhododendron* subsection *Pontica*, a group with a tertiary relict distribution, Mol. Phylogenet. Evol., 33, 389–401, 2004.

594 Miyawaki, A.: A vegetation-ecological view of the Japanese archipelago, Bulletin of the
595   Institute of Environmental Science and Technology, 11, 85–101, 1984.
596 Morlo, M., Gunnell, G. F., and Nagel, D.: Ecomorphological analysis of carnivore guilds in
597   the Eocene through Miocene of Laurasia. In: Carnivoran Evolution: New Views on
598   Phylogeny, Form, and Function, Goswami, A. and Friscia, A. (Eds.), Cambridge
599   University Press, Cambridge, UK, 2010.
600 Neubauer, T. A., Georgopoulou, E., Kroh, A., Harzhauser, M., Mandic, O., and Esu, D.:
601   Synopsis of European Neogene freshwater gastropod localities: updated stratigraphy
602   and geography, Palaeontogia Electronica, 18.1.3T, 1–7, 2015.
603 New, M., Hulme, M. and Jones, P.: Representing Twentieth-Century Space–Time Climate
604   Variability. Part I: Development of a 1961–90 Mean Monthly Terrestrial Climatology,
605   Journal of Climate, 12, 829–856, 1999.
606 New, M., Lister, D., Hulme, M., and Makin, I.: A high-resolution data set of surface climate
607   over global land areas, Climate Research, 21, 1–15, 2002.
608 Peel, M. C., Finlayson, B. L., and McMahon, T. A.: Updated world map of the Köppen-
609   Geiger climate classification., Hydrol. Earth System Sci., 11, 1633–1644, 2007.
610 Quade, J. and Cerling, T. E.: Expansion of C4 grasses in the Late Miocene of Northern
611   Pakistan: evidence from stable isotope paleosols, Palaeogeogr. Palaeoclimatol.
612   Palaeoecol., 115, 91–116, 1995.
613 Rubel, F., Brugger, K., Haslinger, K., and Auer, I.: The climate of the European Alps: Shift of
614   very high resolution Köppen-Geiger climate zones 1800–2100, Meteorologische
615   Zeitschrift, 26, 115–125, 2017. https://doi.org/10.1127/metz/2016/0816.
616 Shevenell, A. E., Kennett, J. P., and Lea, D. W.: Middle Miocene Southern Ocean cooling and
617   Antarctic cryosphere expansion, Science, 305, 1766–1770, 2004.
618 Spicer, R. A.: CLAMP. In: Encyclopedia of Paleoclimatology and Ancient Environments
619   Gornitz, V. (Ed.), Springer, Dodrecht, 2008.
620 Stringer, C. and Andrews, P.: The Complete World of Human Evolution, Thames & Hudson,
621   London, 2011.
622 Strömberg, C.A.E., Werdelin, L., Friis, E.M., Saraç, G.: The spread of grass-dominated
623   habitats in Turkey and surrounding areas during the Cenozoic: phytolith evidence.
624   Palaeogeogr., Palaeoclimatol., Palaeoecol. 250, 18–49, 2007.
625 Suc, J.-P.: Origin and evolution of the Mediterranean vegetation and climate in Europe,
626   Nature, 307, 429–432, 1984.
627 Ter Braak, C.J.F.: Canonical correspondence Analysis: a new eigenvector technique for
628   multivariate direct gradient analysis. Ecology, 67, 1167–1179, 1986.
629 The NOW Community.: New and old worlds database of fossil mammals (NOW). Licensed
630   under CC BZ 4.0 Release 2008. Published on the Internet. Last accessed 23-04-2018.
631   http://www.helsinki.fi/science/now/
632 Ustaoğlu, B.: Comparisons of annual meanprecipitation gridded and station data: An example
633   from Istanbul, Turkey, Marmara Coğrafya Dergisi, 26, 71–81, 2012.
634 Wang, Q., Dilcher, D. L., Lott, T. A.: *Podocarpium* A. Braun ex Stizenberger 1851 from the
635   middle Miocene of Eastern China, and its palaeoecology and biogeography, Acta
636   Palaeobot. 47, 237–251, 2007.
637 Yang, J., Spicer, R. A., Spicer, T. E. V., and Li, C.-S.: 'CLAMP Online': a new web-based
638   palaeoclimate tool and its application to the terrestrial Paleogene and Neogene of North
639   America, Palaeobio. Palaeoen., 91, 163, 2011.
640 Yavuz-Işık, N., Saraç, G., Ünay, E., and de Bruijn, H.: Palynological analysis of Neogene
641   mammal sites of Turkey - Vegetational and climatic implications, Yerbilimeri, 32, 105–
642   120, 2011.
643

Supplementary Material.

S1: A. Number of fossil-taxa (macrofossils and microfossils) from four middle Miocene

localities (including one macrofossil horizon and four pollen zones - PZ) in the Yatağan

Basin.

B. All fossil-taxa recorded from four Yatağan Basin floras (14.8–13.2 Ma; MN6 into MN7–

8).

S2: Köppen-Geiger climate type signatures of all genera represented in micro and macrofloras

of the Yatağan Basin.

S3: Coding of leaf physiognomic characters for morphotypes from three macrofloras. Output

pdf files from online CLAMP analysis (http://clamp.ibcas.ac.cn).

S4: Heat maps showing precise representation of different Köppen-Geiger climate types for

all fossil assemblages.

S5: Köppen signature diagrams excluding cosmopolitan and gymnospermous taxa.

S6: Arboreal to non-arboreal pollen ratios for three sections, of the Yatağan Basin.

**S7**: Modern climate stations comparable to the middle Miocene climate of the Yatağan Basin,

southwestern Anatolia. Climate data from CLIMATE-DATA.ORG (https://sv.climate-

data.org/info/sources/) and Ustaoğlu (2012). Selected Walter-Lieth climate diagrams illustrate

qualitative difference between Euxinian-Hyrcanian and Japanese (Honshu) *Cf* climates.

666 **Tables and Figures**
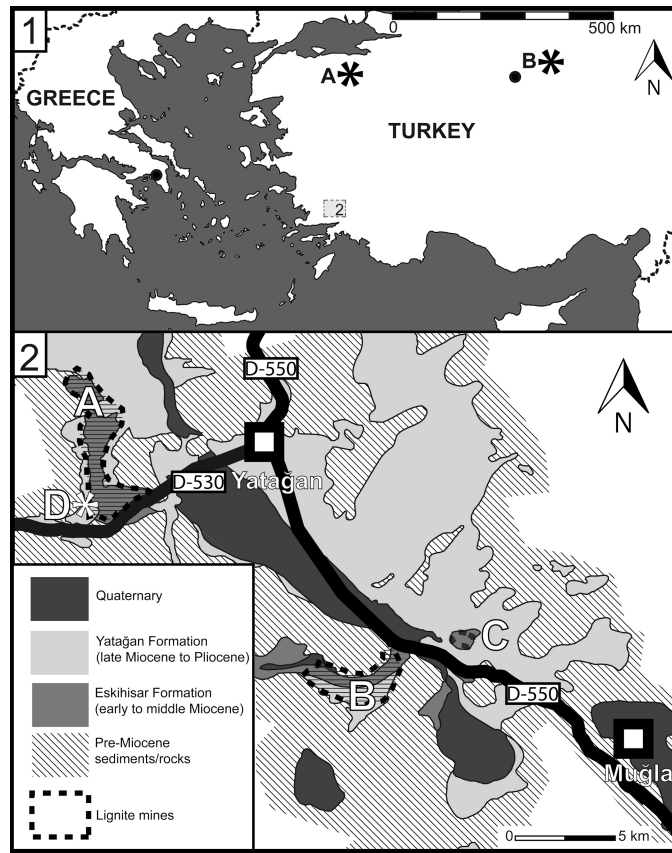
667

668 **Figure 1**. Geographic and regional geologic setting of the Yatağan basin. **1.** Map showing the

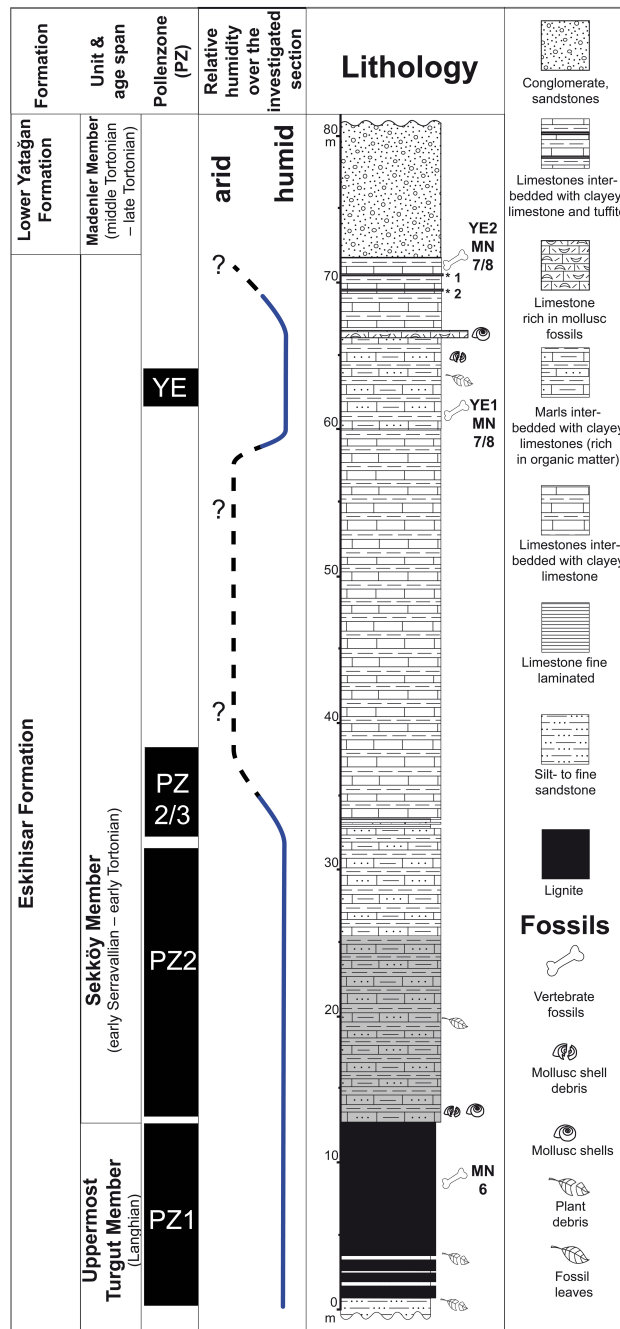669 geographical position of the Yatağan Basin (2) and the MN6 vertebrate fossil localities (*)

670 Paşalar (A) and Çandir (B). **2.** Simplified regional geological map of the Yatağan Basin based

671 on Becker-Platen (1970) and Atalay (1980); lignite mines Eskihisar (A), Tınaz (B),

672 Salihpaşalar (C); vertebrate fossil locality (*) Yeni Eskihisar MN7/8 (D).

673

674

Figure 2. Generalized lithostratigraphic column for the Eskihisar lignite mine and pollen

zones (PZ). The main part of the investigated plant macrofossils originates from ca 10 m thick

deposits overlying the exploited lignite seams (part of the section highlighted in grey

corresponding to PZ 2). Yeni Eskihisar 2 (YE2) and Yeni Eskihisar 1 (YE1) vertebrate fossil

localities (Becker-Platen et al. 1977). Radiometrically dated tuff layers (*), 1* 11.2 ± 0.2 Ma,

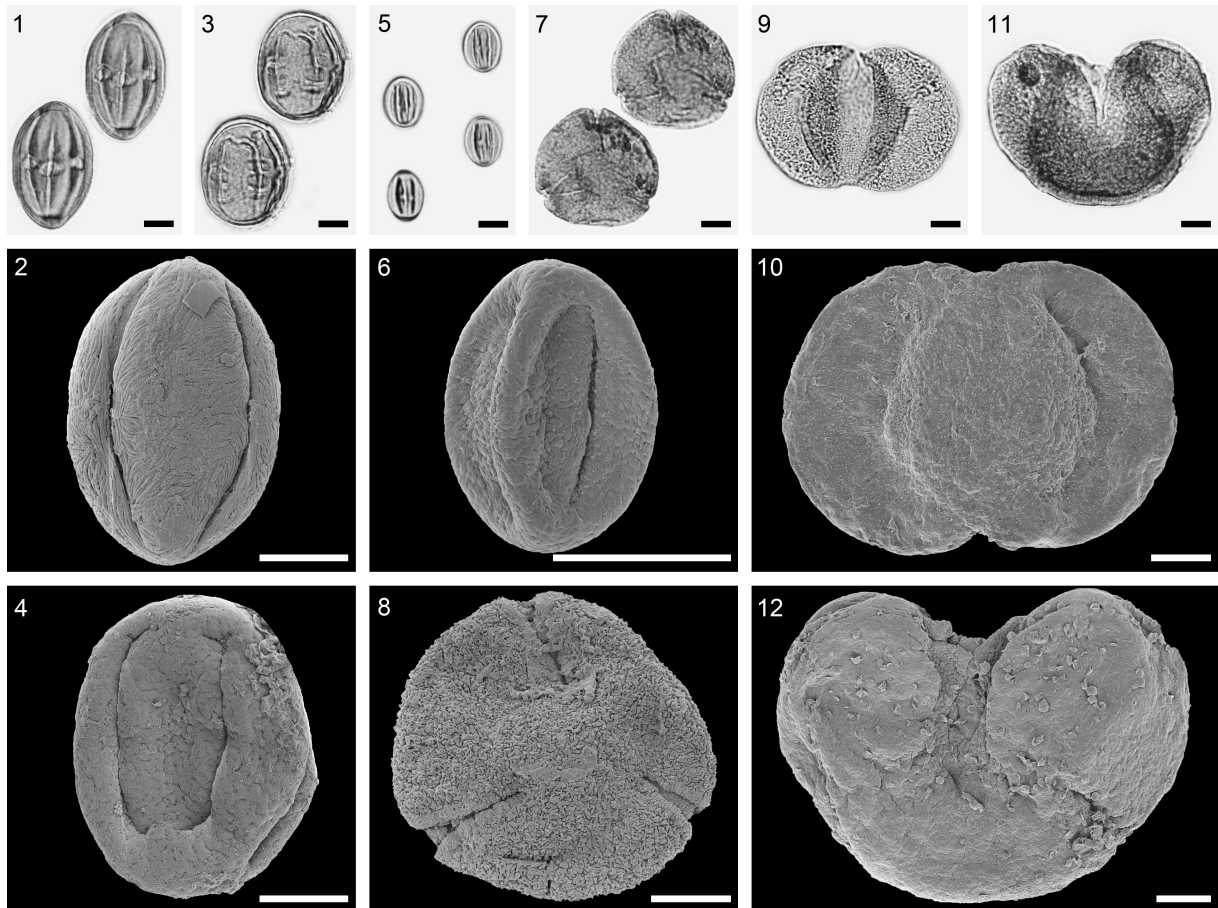2* 13.2 ± 0.35 Ma (Becker-Platen et al. 1977).

681
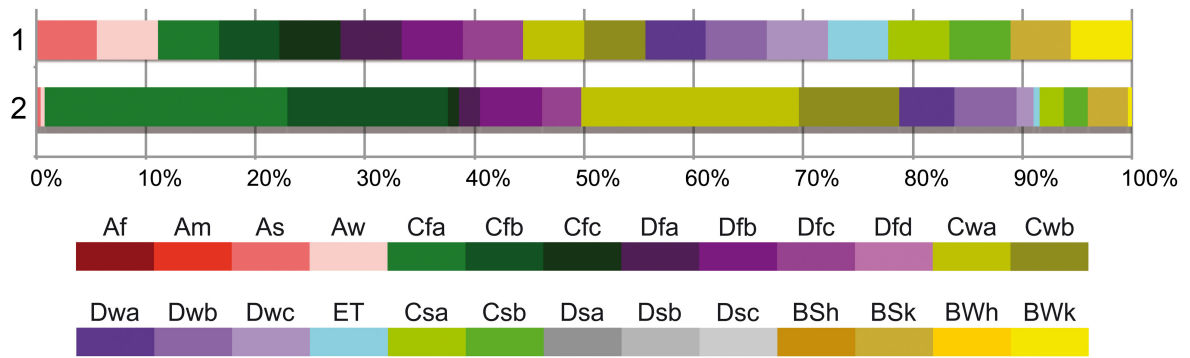
Figure 3. Köppen signal for genus *Tilia* extracted from 26 extant species. **1**. Köppen-Geiger climates in which *Tilia* is present. **2**. Combined Köppen signature of all 26 extant *Tilia* species.

Figure 4. Selected pollen grains LM (1, 3, 5, 7, 9, 11) and SEM (2, 4, 6, 8, 10, 12) micrographs of the same fossil pollen grain of the Eskihisar (E)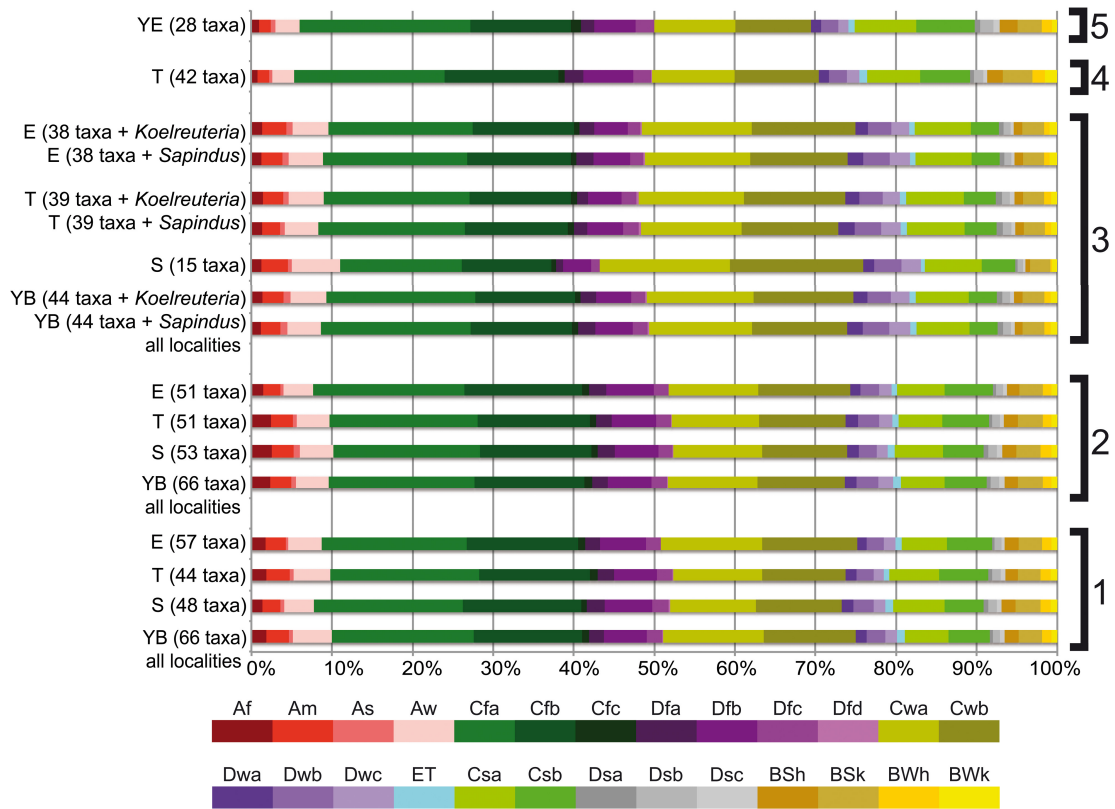, Tınaz (T), and Salihpaşalar (S) sections. **1–2**. *Nitraria* sp., EV (E, S153567). **3–4**. Sapotaceae gen. indet., EV (T, S143604). **5–6**. *Decodon* sp., EV (S, S153635). **7–8**. *Fagus* sp., PV (T, S143621). **9–10**. *Cathaya* sp., (9) PV, (10) PRV (S, S153632). **11–12**. *Cedrus* sp., EV (E, S153590). EV = equatorial view, PV = polar view, PRV = proximal view. Scale bar = 10μm (1–12).

Figure 5. Köppen signals for the Yatağan Basin floras. **1.** Pollen zone (PZ) 1 (MN6; 14.95–13.9 Ma) of the Eskihisar (E), Tınaz (T), and Salihpaşalar (S) localities and the combined signal of all present taxa from PZ 1 of the three Yatağan Basin localities (YB). **2.** PZ 2 (MN6) of E, T, S, YB. **3.** Macrofossil (MF) assemblages (same level as PZ 2) of E, T, S. **4.** PZ 2/3 of T. (younger than Yeni Eskihisar vertebrate locality). **5.** Yeni Eskihisar vertebrate locality pollen assemblage (MN7/8, younger than radiometric age 13.2 Ma).

703
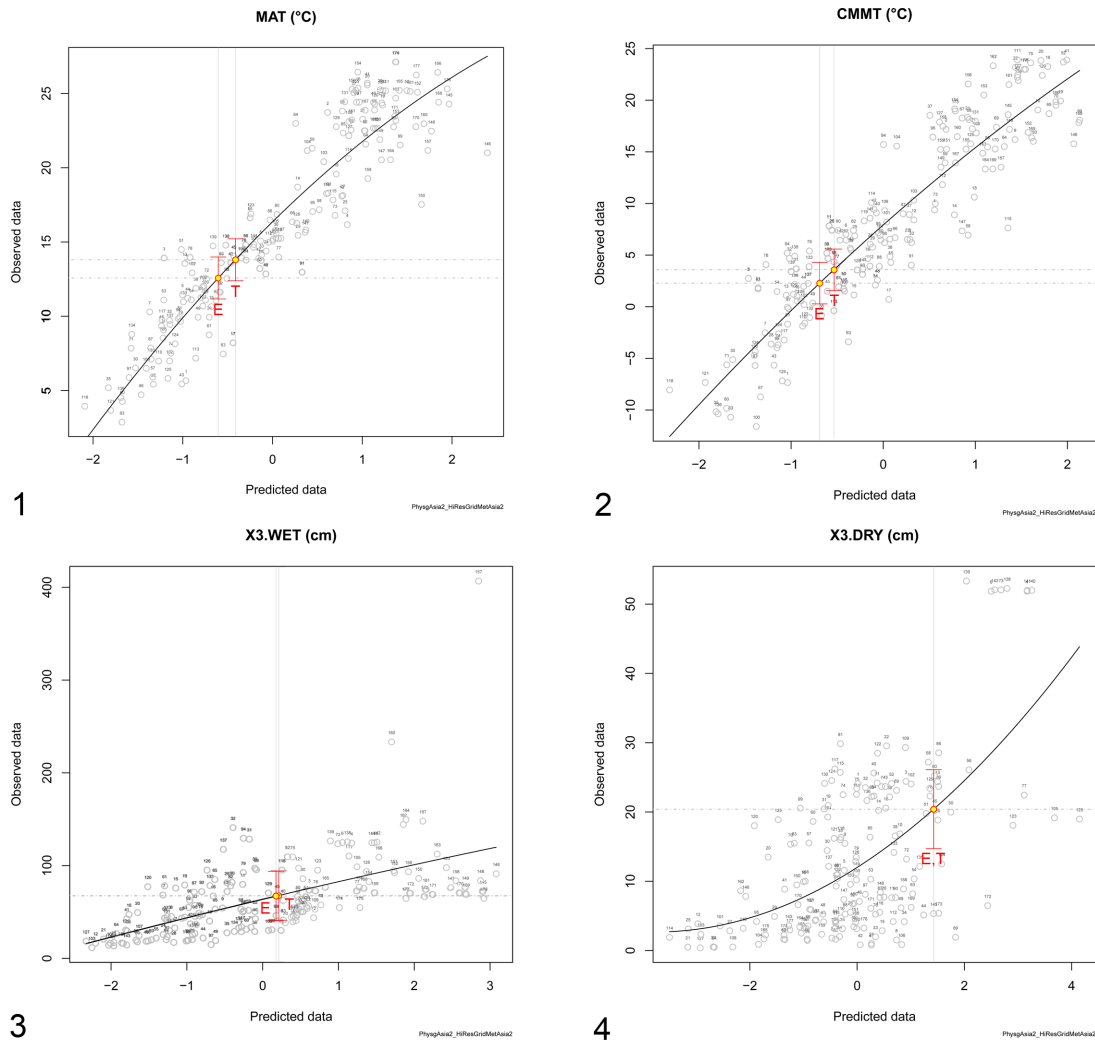
Figure 6. CLAMP climate inference for the macrofossil assemblage of (E) Eskihisar and (T)

Tınaz (same level as PZ 2). **1.** Mean annual temperature (MAT). **2.** Coldest month mean

temperature (CMMT). **3.** Precipitation of the three wettest months. **4.** Precipitation of the

three driest months.

Table 1

Latest occurrence W Eurasia	Fossil-taxon (genus level)	wEUR[f]	EA	eNA	wNA	SA	AF	AUS
	Ephedra	+	+	+	+	+	+	
Pliocene?[a]	*Glyptostrobus*		+					
Taxodium-type, < 0.1 Ma[a]	*Taxodium*			+	+			
0.5-0.4 Ma[a]	*Cathaya*		+					
	Cedrus	+	+					
	Picea	+	+	+	+			
	Pinus	+	+	+	+			
0.4-0.3 Ma[a]	*Tsuga*		+	+	+			
	Acer	+	+	+	+			
late Pliocene[b]	*Ailanthus*		+					
	Alnus	+	+	+	+	+		
no data	*Apios*		+	+				
	Betula	+	+	+	+			
	Buxus	+	+	+	+	+	+	
	Buxus (balearica type)	+	+					
	Carpinus	+	+	+				
< 0.1 Ma[a]	*Carya*		+	+				
	Castanea	+	+	+				
Pliocene[c]	*Cedrelospermum*†	+	+		+			
	Celtis	+	+	+	+	+	+	+
	Centranthus	+	+					
	Corylus	+	+	+	+			
Pleistocene[d]	*Decodon*			+				
	Drosera	+	+	+	+	+	+	+
	Erica	+					+	
	Erodium	+	+	+	+	+	+	+
0.6 Ma[a]	*Eucommia*		+					
	Euphorbia	+	+	+	+	+	+	+
	Fagus	+	+	+				
	Fraxinus	+	+	+	+			
	Ilex	+	+	+	+	+	+	+
	Juglans	+	+	+	+	+		
	Linum	+	+	+	+	+	+	+
	Liquidambar	+	+	+				
	Lonicera	+	+	+	+			
	Ludwigia	+	+	+	+	+	+	+
Pliocene[d]	*Mahonia*		+					
	Nitraria	+	+				+	+
	Ostrya	+	+	+				
	Parrotia	+						
	Persicaria	+	+	+	+	+		
	Phragmites	+	+	+	+	+	+	+
no data	*Picrasma*		+	+	+	+		
Pleistocene[e]	*Podocarpium* †	+	+					
	Polygonum	+	+	+	+			
	Populus	+	+	+	+			
	Pterocarya	+	+					
	Quercus	+	+	+	+	+		
	Rumex	+	+	+	+	+	+	+
	Salix	+	+	+	+	+		
	Scabiosa	+					+	
	Smilax	+	+	+	+	+	+	+
14.8-13.8 Ma	*Smilax (havanensis* group*)*			+		+		
	Sorbus	+	+	+	+			
	Sparganium	+	+	+	+			+
	Tilia	+	+	+	+			
	Typha	+	+	+	+	+	+	+
	Ulmus	+	+	+	+			
	Viburnum	+	+	+	+	+		
	Zelkova	+	+					
	No. of genera/region	48	54	44	36	21	16	13
		wEUR[f]	EA	eNA	wNA	SA	AF	AUS

Table 1. Genus-level biogeographic affinities of fossil-taxa of the Yatağan Basin floras.

[a]Magri et al., 2017; [b]Corbett & Manchester, 2004; [c]Jia et al., 2015; [d]Martinetto, 2001; [e]Wang et al., 2007; [f]including northern Africa; † extinct genus.

713   wEUR = western Eurasia, EA = East Asia, eNA = eastern North America, wNA = western

714   North America, SA = South America, AF = Africa (excluding northern Africa), AUS =

715   Australia.

716

Table 2

Pollen Zone	AP	NAP	
Hüssamlar	90	10	16.8 Ma
Kultak	90	10	MN5
Karacaağaç	96	4	
Tınaz PZ1	75,00	25,00	14.8 Ma
	94,20	5,80	
	0,00	0,00	MN6
	0,00	0,00	
	75,58	24,42	
	85,00	15,00	
	0,00	0,00	
Tınaz PZ2	54,13	45,87	
	89,22	10,78	
	62,04	37,96	
	86,82	13,18	
	28,66	71,34	
	46,04	53,96	
	0,00	0,00	13.9 Ma
Tınaz PZ2-3	19,01	80,99	(?)MN7+8
	0,00	0,00	*
	50,44	49,56	MN7+8
Yenieskihisar	67,00	33,00	13.2 Ma

* = perhaps linked with 13.9-13.8 Ma cooling event
(Holbourn et al., 2014)
AP = arboreal pollen (angiosperms)
NAP = non-arboreal pollen (angiosperms)
wavy line = profiles separated by tens of meters
of sediment barren of pollen

717

718 **Table 2**. Arboreal to non-arboreal pollen ratios in southwestern Anatolia across the MCO,

719 MMCT and subsequent cooling phase.

720

Table 3

Descripton of Köppen-Geiger climate symbols and defining criteria			
1st	2nd	3rd	Description and criteria
A			equatorial / tropical ($T_{cold} \geq 18°C$)
	f		rainforest, fully humid ($P_{dry} \geq 60mm$)
	m		monsoonal (not Af & $P_{dry} \geq 100$-MAP/25)
	s		savannah with dry summer ($P_{sdry} < 60$ mm)
	w		savannah with dry winter ($P_{wdry} < 60$ mm)
B			arid (MAP <10 x $P_{threshold}$)
	W		desert (MAP <5 x $P_{threshold}$)
	S		steppe (MAP $\geq$5 x $P_{threshold}$)
		h	hot arid (MAT $\geq 18°C$)
		k	cold arid (MAT <18°C)
C			warm temperate/temperate ($T_{hot} > 10°C$ & $0°C< T_{cold} < 18°C$)
D			snow / cold ($T_{hot} > 10°C$ & $T_{cold} \leq 0°C$)
	s		summer dry ($P_{sdry} < 40$ & $P_{sdry} < P_{wwet}/3$)
	w		winter dry ($P_{wdry} < P_{swet}/10$)
	f		fully humid / without a dry season (not s or w)
		a	hot summer ($T_{hot} \geq 22°C$)
		b	warm summer (not a & $1 \leq T_{mon}10 < 4$)
		c	cool / cold summer (not a or b & $T_{mon}10 \geq 4$)
		d	extremely continental / very cold winter (not a or b & $T_{cold} < -38°C$)
E			polar ($T_{hot} < 10°C$)
	T		polar tundra ($T_{hot} \leq 10°C$)

Table 3 Description of Köppen-Geiger climate symbols and defining criteria (Kottek et al., 2006; Peel et al. 2007). MAP = mean annual precipitation, MAT = mean annual temperature, T_{hot} = temperature of the hottest month, T_{cold} = temperature of the coldest month, T_{mon10} = number of months where the temperature is above 10°C, P_{dry} = precipitation of the driest month, P_{sdry} = precipitation of the driest month in summer, P_{wdry} = precipitation of the driest month in winter, P_{swet} = precipitation of the wettest month in summer, P_{wwet} = precipitation of the wettest month in winter, $P_{threshold}$ = varies according to the following rules (if 70% of MAP occurs in winter then $P_{threshold} = 2$ x MAT, if 70% of MAP occurs in summer then $P_{threshold} = 2$ x MAT + 28°, otherwise $P_{threshold} = 2$ x MAT + 14). Summer (winter) is defined as the warmer (cooler) six months period of ONDJFM and AMJJAS.

733